



Influence of lateral displacement on strip shape during cold rolling

Zhong-kai Ren^{1,2,3} · Hong Xiao^{1,2} · Hong-biao Xie^{1,2} · Xiao Liu^{1,2}

Received: 27 May 2017 / Revised: 27 September 2017 / Accepted: 10 October 2017 / Published online: 31 August 2018
© China Iron and Steel Research Institute Group 2018

Abstract

The theory of metal plastic deformation is an important part of the strip shape control theories. In order to control the shape and gauge accurately during cold thin strip rolling, the mechanism of the metal lateral flow must be revealed clearly. Therefore, the lateral displacement of thin strip was studied by the grid method. Those grids with a line thickness of 10 μm and clear boundaries were successfully manufactured on the strip surface using lithography. Then, the effects of reduction, front and back tension, and taper angle of the first intermediate roll on the metal lateral flow were studied. The strip shape was calculated with and without considering the lateral displacement; furthermore, the calculations were compared with the measured results. The results show that the calculations with considering the lateral displacement are closer to the measured results. In addition, the comparison of finite element analysis results with the experimental results indicates that the test method was reliable.

Keywords Thin strip · Lithography technology · Lateral displacement · Strip shape · Experimental research · Finite element simulation · Cold rolling

1 Introduction

The theory of metal plastic deformation is the main component of the strip shape control theories, mainly studying the mechanism of metal permanent deformation during the rolling. At the beginning of the study, Karman [1] and Orowan [2] treated it as a plane strain problem neglecting the metal lateral flow along the width direction. However, the metal deformation not only elongates along the rolling direction, but also flows along the width direction. Some scholars have done a lot of theoretical analysis concerning the mechanism of three-dimensional deformation. Currently, there are three general methods for analyzing the three-dimensional deformation of a workpiece, including

finite difference method [3–5], finite element method [6–9], and energy method [10–15]. Other scholars make efforts to study the plastic deformation of the strip by experiments. For the plastic flow of thick-walled tubes, MacGregor et al. [16] obtained the distributions of the vertical, axial, and lateral strains by studying both square and circular grids scribed on the side surface of the workpiece. Burger and Gomide [17] predicted the three-dimensional strain distribution of an aluminum plate in hot rolling process by photoplastic simulation. Based on viscoplasticity, Thomson and Brown [18] investigated the deformation mechanism of the aluminum strip during cold rolling. The influence on the deformation of reduction, front and back tension, the ratio of roll diameter to specimen thickness, and lubrication was researched. Unfortunately, experimental studies on the metal lateral flow for thin strip rolling have not been found.

The grid method is a most comprehensive experimental method for studying the plastic deformation of the metal. The grids on the surface of the specimen can be manufactured by the engraving method, the screen printing method, etc. Nonetheless, the line thickness of the grid prepared by the existing methods is about 0.2 mm, and its boundaries are not clear. The magnitude of the lateral displacement is at the micron range during cold thin strip

✉ Hong Xiao
xhh@ysu.edu.cn

¹ College of Mechanical Engineering, Yanshan University, Qinhuangdao 066004, Hebei, China

² National Engineering Research Center for Equipment and Technology of Cold Strip Rolling, Yanshan University, Qinhuangdao 066004, Hebei, China

³ College of Mechanical Engineering, Taiyuan University of Technology, Taiyuan 030024, Shanxi, China

rolling. If the above methods are used to prepare the grids, the measurement error of the lateral displacement will be very large, and the displacement variation even cannot be measured. In order to study the lateral displacement accurately, the grid with a line thickness of 10 μm and clear boundaries was successfully manufactured on the surface of 304-stainless steels by lithography. On the basis of this, the effects of reduction, front and back tension, and taper angle of the first intermediate roll on the metal lateral flow were studied. Moreover, the strip shape was calculated with and without considering the lateral displacement, and the calculations were compared with the measured results.

2 Experimental apparatus and methods

2.1 Preparation of specimen

As shown in Fig. 1a, a grid with line thickness of 10 μm and clear boundaries was successfully manufactured on the strip surface by lithography. The grid sections were shown to be very clear at a magnification of 50 \times , as shown in Fig. 1b. The manufacturing process for this is as follows.

1. Preparation of the strip: Each strip was cut into a 250-mm-long specimen, and both ends were cut into semicircular shapes.
2. Spin coating treatment: BP-212 series positive photoresist was coated to the strip surface with the KW-4A spin coating machine.
3. Solidification treatment: Each specimen was solidified in a drum wind drying oven.
4. Exposure processing: A mask with a line thickness of 10 μm and grids of 2 mm \times 0.3 mm was installed on a BG-401A exposure machine. Then, it is exposed at room temperature for 20 s.
5. Development processing: The development was carried out by using tetramethylammonium hydroxide with a concentration of 1.04 mol/L.
6. Solidification strengthening: In order to improve the adhesion of the photoresist on the strip surface, the specimen was again placed in the drum wind drying oven.

2.2 Cementation of specimen

During strip rolling process, it is necessary to apply the tension. Hence, those specimens will be glued together with leading tapes. Before cementation, the specimen and leashes were clamped on the special platform to ensure that they are in the same plane and parallel to each other. After adjusting the position between each other, they were cohered with GLH-302 adhesive.

2.3 Rolling experiment

After 24 h of cementation, the rolling experiment was carried out. Various workpieces were rolled by a 20-high mill in laboratory. The 20-high mill rolls system arrangement is shown in Fig. 2, and its primary technological parameters are listed in Table 1. For researching the regularity of lateral flow during cold strip rolling, the effects of reduction, front and back tension, and taper angle on the metal lateral flow were studied.

2.4 Measurement of exit thickness and lateral displacement and strip shape

Before rolling, the initial thickness distribution of the workpiece was measured by the MDH-25M caliper with a precision of 0.1 μm . Measurement was taken at one location every 5 mm, and the average value of three measurements at each position was obtained. After several

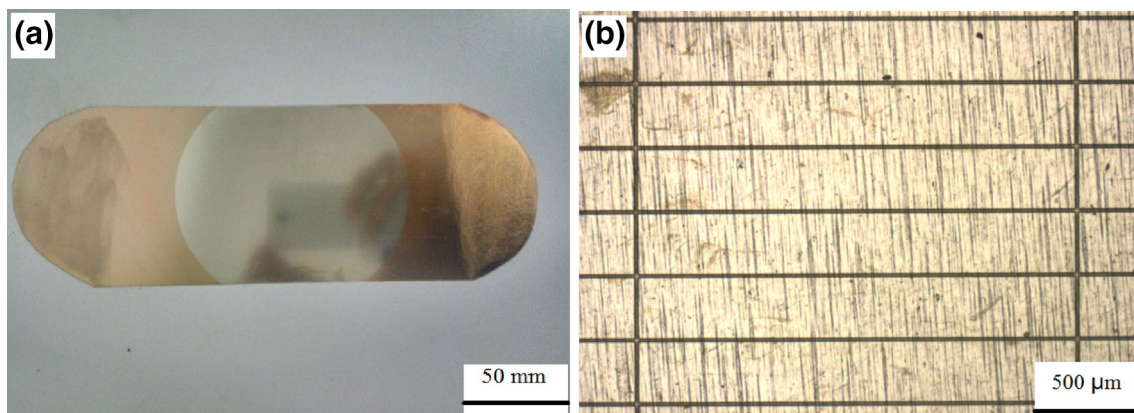


Fig. 1 Specimen with a diameter of 10 μm (a) and enlarged partial view (b)

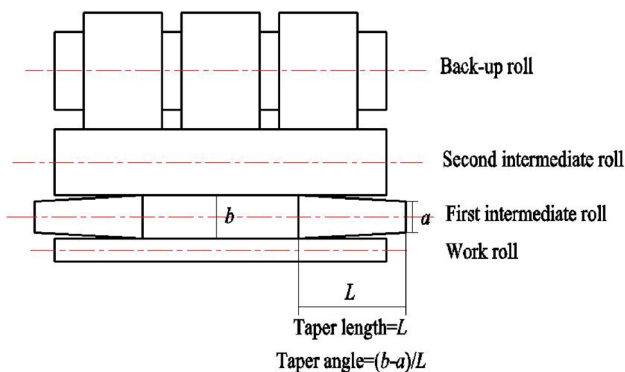


Fig. 2 20-high mill rolls system arrangement

Table 1 Primary technological parameters of 20-high mill

Parameter	Value
Work roll/(mm × mm)	$\phi 12 \times 160$
First intermediate roll/(mm × mm)	$\phi 22 \times 170$
Second intermediate roll/(mm × mm)	$\phi 36 \times 160$
Back-up roll/(mm × mm)	$\phi 60 \times 40 \times 3$
Strip width/mm	85
Strip thickness/mm	0.2, 0.3
Strip yield strength/MPa	309, 315
Taper angle	0.001, 0.002, 0.003
Taper length/mm	50, 60

measurements, it was found that the initial crown of the specimen is almost zero; thus, the initial thickness is assumed to be a uniform distribution. After rolling, the distribution of the exit thickness was measured in the same manner.

In this paper, the lateral displacement is the amount of change in the corresponding grid coordinates before and after rolling. And, it is defined that the outside along the width direction of the strip is the positive direction and the

inside is the negative direction. The lateral displacement was measured in two steps, and the displacement of the edge was measured directly, while the remaining positions were measured indirectly. Before and after rolling, the distance from the edge of the strip to the nearest grid line was measured. Afterward, the variation in the lateral displacement at the edge was obtained by determining a difference between the two measurements. The remaining positions were measured as follows: Pictures were taken every 2 mm using an electron microscope at a magnification of 50×. These pictures were pieced together with Photoshop software. Afterward, as shown in Fig. 3a, the spliced picture was measured using the AutoCAD software. Specifically, as shown in Fig. 3b, two borderlines were drawn at the required position to ensure that they coincide with the boundaries of the grid line. Then, the symmetry line of the boundaries was taken as the center line of the grid line. And, the center line of the strip was used as a datum. Based on the datum, the distance was measured every 4 mm. Finally, the actual value of the lateral displacement was obtained from the measured value and the magnification times.

After measurement of lateral displacement, the specimen was cut into long narrow strips by wire-electrode cutting, including two 4.5 mm × 25 mm strips at the edge of the workpiece and nineteen 4 mm × 25 mm strips in the middle. And then, the strip shape was measured by using the same method of measuring the lateral displacement.

3 Results and discussion

3.1 Influence of reduction on metal lateral flow

In this experiment, strip entry thickness is 0.3 mm, and strip width is 85 mm; both front and back tensions are 118 MPa; taper angle is 0.003, and taper length is 50 mm;

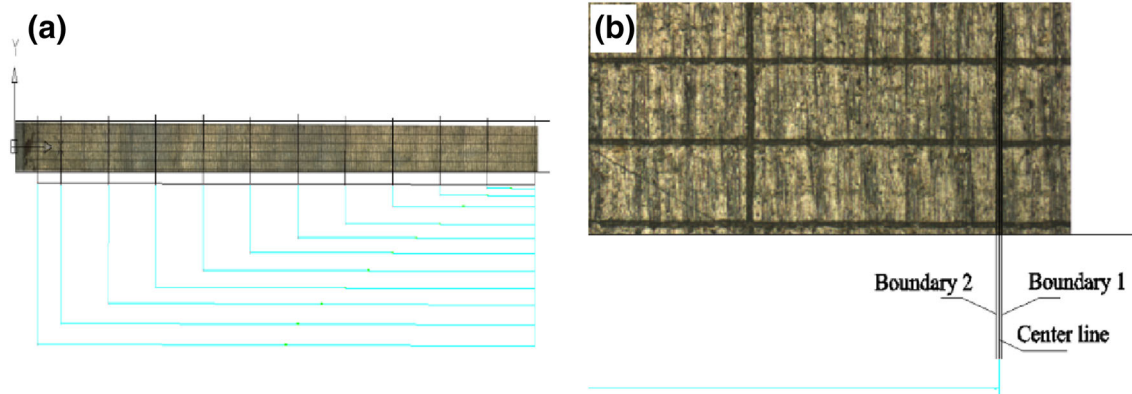


Fig. 3 Measurement of lateral displacement. a Complete diagram of specimen; b drawing of partial enlargement

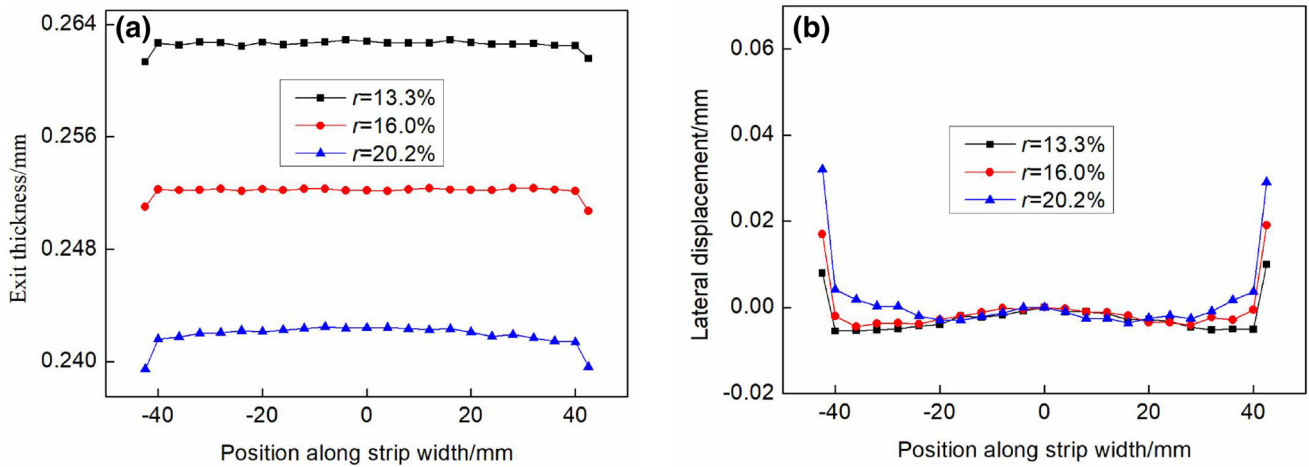


Fig. 4 Measurements of exit thickness (a) and lateral displacement (b) under different reductions r

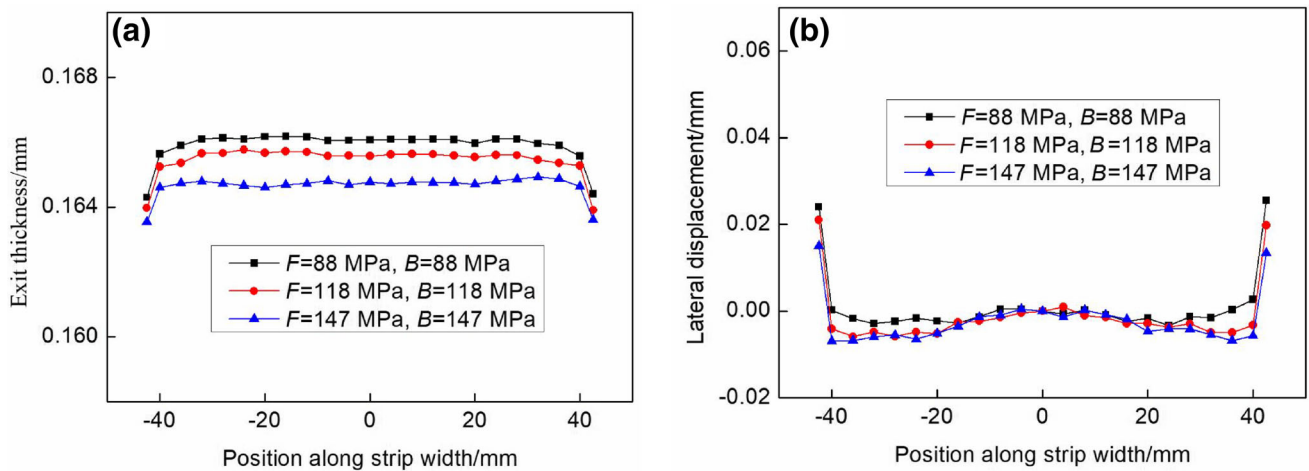


Fig. 5 Measurements of exit thickness (a) and lateral displacement (b) under different front tensions F and back tensions B

and the reductions are 13.3%, 16.0% and 20.2%, respectively. The measurements of the exit thickness and the lateral displacement are shown in Fig. 4. As the reduction increases, it can be found that the thinning phenomenon becomes more serious at the edge, and the lateral displacement is changed from negative to positive. This is because the pressure between rolls increases as the reduction increases, which causes the raise of the deflection of the work roll.

3.2 Influence of front and back tensions on metal lateral flow

In this experiment, strip entry thickness is 0.2 mm, and strip width is 85 mm; the reduction is approximately 17.7%; taper angle is 0.002, taper length is 50 mm; and front and back tensions are 88 MPa/88 MPa, 118 MPa/118 MPa, and

147 MPa/147 MPa, respectively. The measurements of the exit thickness and the lateral displacement are shown in Fig. 5. As the front and back tensions increase, the thinning phenomenon becomes lighter at the edge, and the lateral displacement changes inversely from positive to negative. Owing to the increase in the front and back tensions, on one hand, both the rolling force and the deflection of the work roll decrease; on the other hand, it is helpful to the plastic deformation of the metal along the rolling direction, but restricts the flow of the metal along the width direction.

3.3 Influence of taper angle of first intermediate roll on metal lateral flow

In this experiment, strip entry thickness is 0.3 mm, and strip width is 85 mm; front and back tensions are 78 MPa/

78 MPa; the reduction is approximately 16.5%; taper length is 50 mm, and taper angles are 0.001, 0.002, and 0.003, respectively. The measurements of the exit thickness and the lateral displacement are shown in Fig. 6. As the taper angle decreases, the thinning phenomenon becomes more serious at the edge and the lateral displacement is changed from negative to positive. In addition, there is a clear edge buckle, when the taper angle is 0.001. Because the taper angle decreases, the contact pressure between work roll and first intermediate roll gradually increases, which causes the increase in the deflection of the work roll.

As a result, with the increase in the reduction and the decrease in the taper angle and tension, the thinning phenomenon becomes more serious at the edge and the lateral displacement is changed from negative to positive. This is due to the increase in the contact pressure between rolls, which causes the increase in the deflection of the work roll. On one hand, the increase in the deflection of the work roll

leads to the increase in the edge drop of the strip. On the other hand, the lateral resistance of the metal at the edge area is much smaller than that inside. Therefore, there is a significant lateral flow at the edge area. Furthermore, the lateral resistance is zero at the extreme edge; thus, there is always an abrupt change. As for the negative lateral displacement under the condition of small reduction, or large taper angle or large tension, the effect of the tension on the metal flow is greater than that of the edge drop of the strip. In order to make the tension distribution more uniform, the metal flows from a region with small tension to a region with large tension.

3.4 Influence of flatness defects on metal lateral flow

As shown in Fig. 7, under the conditions of front and back tensions of 78 MPa/78 MPa, the taper length of the first

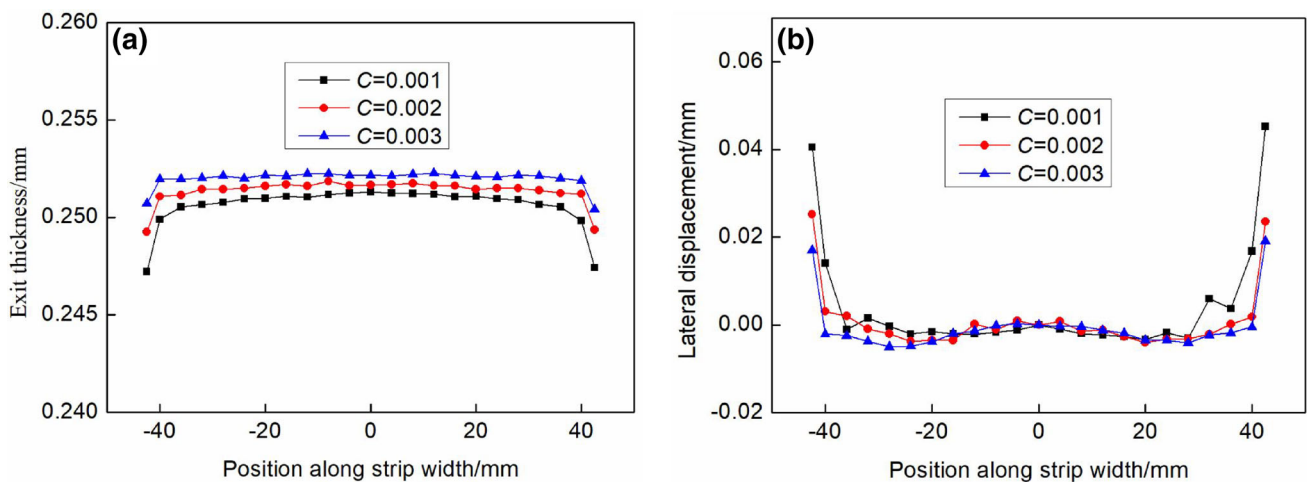


Fig. 6 Measurements of exit thickness (a) and lateral displacement (b) under different taper angles C

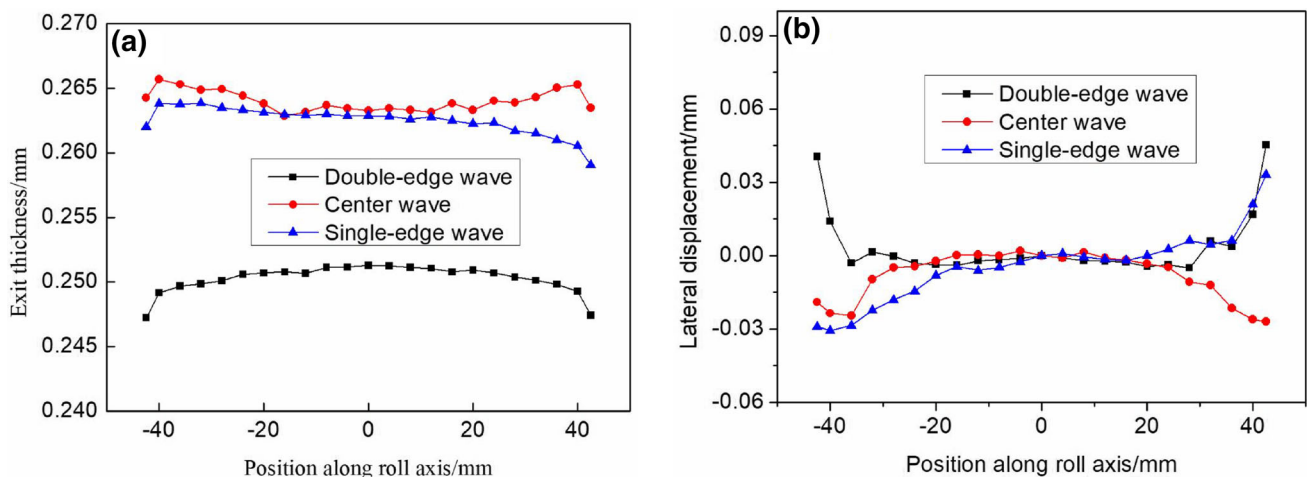


Fig. 7 Measurements of exit thickness (a) and lateral displacement (b) with different shape defects

intermediate roll of 50 mm, taper angle of 0.001, and the reduction of 16.9%, there is an obvious double-edge buckle and the metal is more likely to flow in the positive direction. Under the conditions of front and back tensions of 78 MPa/78 MPa, the taper length of 60 mm, taper angle of 0.003, and the reduction of 12.3%, there is an obvious center buckle and the metal is more likely to flow in the negative direction. Under the conditions of front and back tensions of 78 MPa/78 MPa, the taper length of 50 mm, taper angle of 0.002, and the reduction of 11.7%, there is an obvious single-edge buckle and the metal is more likely to flow in the positive direction at the side of buckle.

3.5 Influence of lateral displacement on strip shape

For further analyzing the influence of the lateral displacement on the strip shape, the strip shape was calculated with and without considering the lateral flow of the metal, and the calculated results were compared with the measurements.

The deformation of the strip is close to the plane deformation regardless of the lateral displacement. According to the incompressibility condition of the volume, the relationship between longitudinal extension and height compression is as follows:

$$\frac{L(x)}{l(x)} = \frac{h(x)}{H(x)} \tag{1}$$

where $H(x)$ is the sectional shape of the strip at the entrance; $L(x)$ is the original length corresponding to each point along the cross section; $h(x)$ is the sectional shape of the strip at the exit; and $l(x)$ is the length corresponding to each point along the cross section after rolling.

With considering the lateral displacement, the width of the strip shown in Fig. 8 is analyzed. According to the incompressibility condition of the volume, the equation is given:

$$H(x)L(x)\Delta x = h(x)l(x)\Delta x \left[1 + \frac{du(x)}{dx} \right] \tag{2}$$

where

$$u(x) = \frac{u'(x)}{M} \tag{3}$$

$$u'(x) = B'_i(x) - B_i(x) \tag{4}$$

$u(x)$ is the lateral displacement at the exit of the deformation zone; $B'_i(x)$ is the measured distance at the exit of

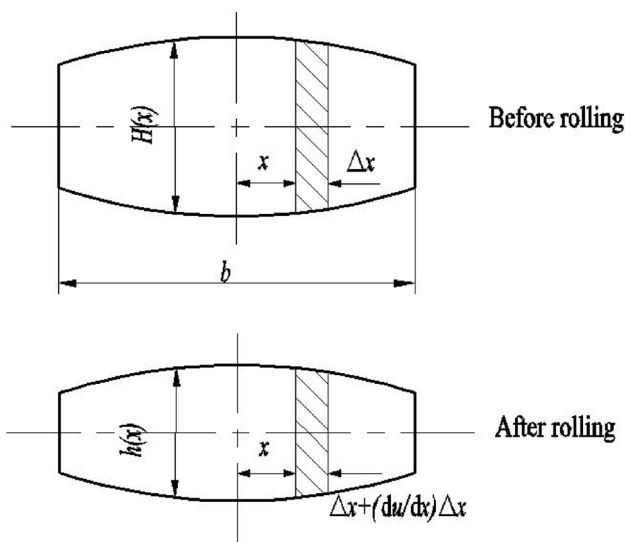


Fig. 8 Sketch of spread

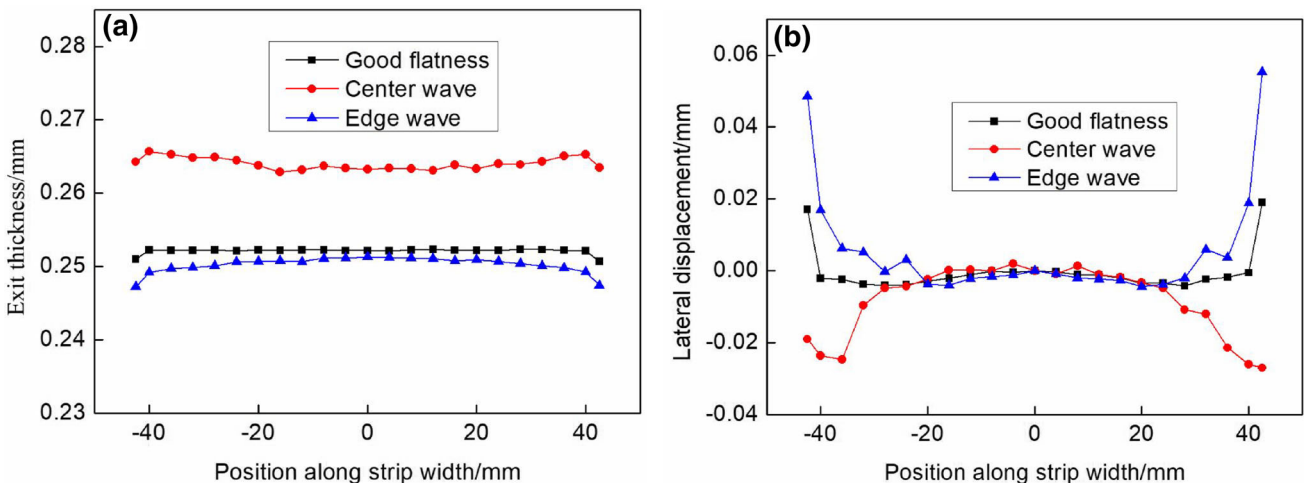


Fig. 9 Measurements of exit thickness (a) and lateral displacement (b) with different conditions

the deformation zone, which is from the center line of the i -th grid to the datum line shown in Fig. 3; $B_i(x)$ is the known distance at the entrance, which depends on the datum line and the grid size on the surface of the mask; $u'(x)$ is the lateral displacement measured with AutoCAD software at the exit; and M is the total magnification time.

The three cases mentioned above were analyzed and contrasted, including good flatness, edge buckle and center buckle of rolled strip. Figure 9 shows the exit thickness and the lateral displacement under different conditions. The comparisons between the measured strip shape and the calculations by Eqs. (1) and (2) are shown in Fig. 10. The results show that the calculations without considering the lateral displacement reveal obvious shape defects, and the calculations considering the lateral displacement are closer to the measured results. Thus, the effect of the lateral displacement on the strip shape cannot be neglected.

4 Finite element simulation analysis

The finite element analysis (FEA) was carried out for the above experimental results. As shown in Fig. 11, since the rolls system is symmetrical, a quarter symmetry model was used for analysis. The monoblock housing is simplified to be a rigid structure in this model, as it normally has the highest mill modulus. The rolls system and strip are modeled as elastic and elastic–plastic bodies, respectively. In order to obtain reliable results and save computing time, it is essential to refine mesh elements near the contact region.

The element type of rolls system and strip is C3D8R. The element type of the monoblock housing is R3D4. The thickness of the workpiece is divided into four layers of square elements. In the model, the true stress–strain curve of the strip is transformed according to the measured data via a tensile test. The yield criterion is modeled using the Mises yield criterion. In addition, the friction between the work roll and the strip is modeled using the Coulomb friction law. As lubricants are used in the experiments, the coefficient of friction is assumed to be 0.08 [19]. The elastic modulus and Poisson's ratio of the work roll are 236 GPa and 0.3, respectively. And the elastic modulus and Poisson's ratio of the other rolls are 207 GPa and 0.25, respectively.

When the experimental conditions are analyzed based on finite element analysis, simulations are carried out under a certain experimental condition twice with different element sizes. In the first simulation, the thickness of the strip is divided into five layers. And in the second simulation, the thickness of the strip is divided into four layers. The comparison result is shown in Fig. 12; it is found that there is a slight difference. However, it will greatly increase the

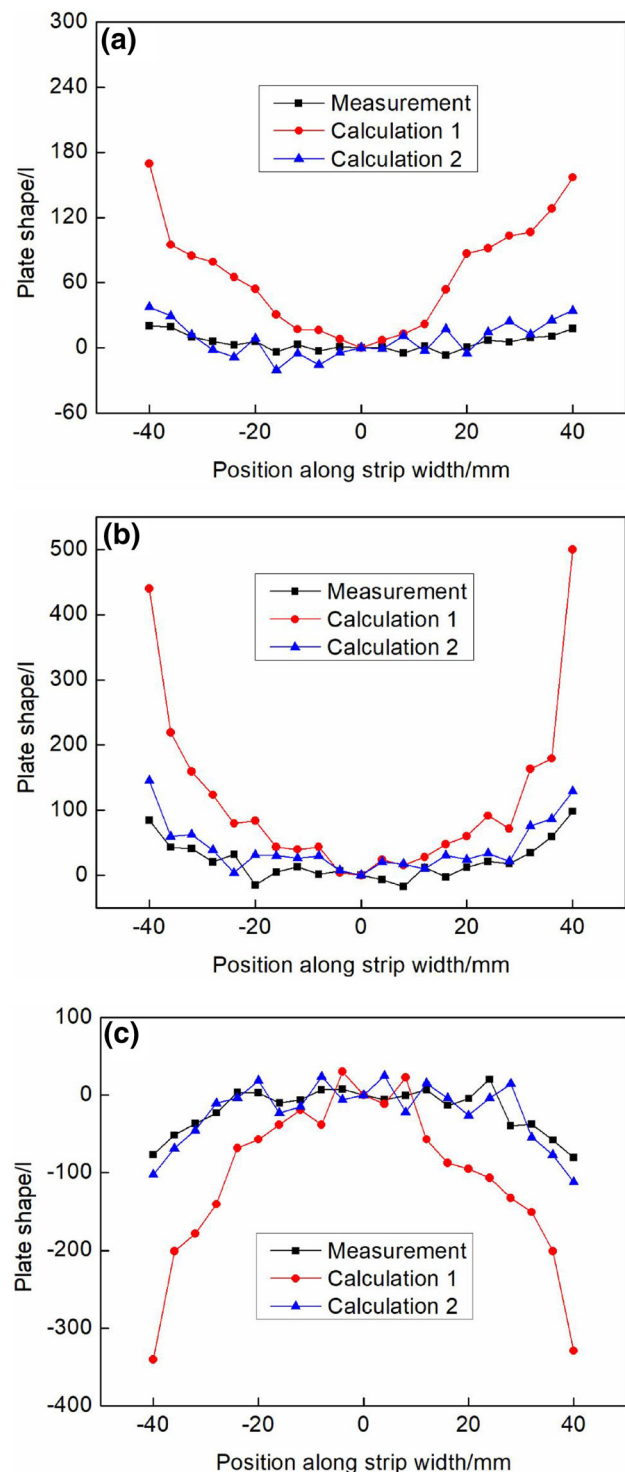


Fig. 10 Comparison between calculated and measured strip shapes. **a** Good flatness; **b** edge buckle; **c** center buckle

calculation time, when the thickness of the strip is divided into five layers. In summary, the simulation results are accurate and reliable, when the thickness of the strip is divided into four layers.

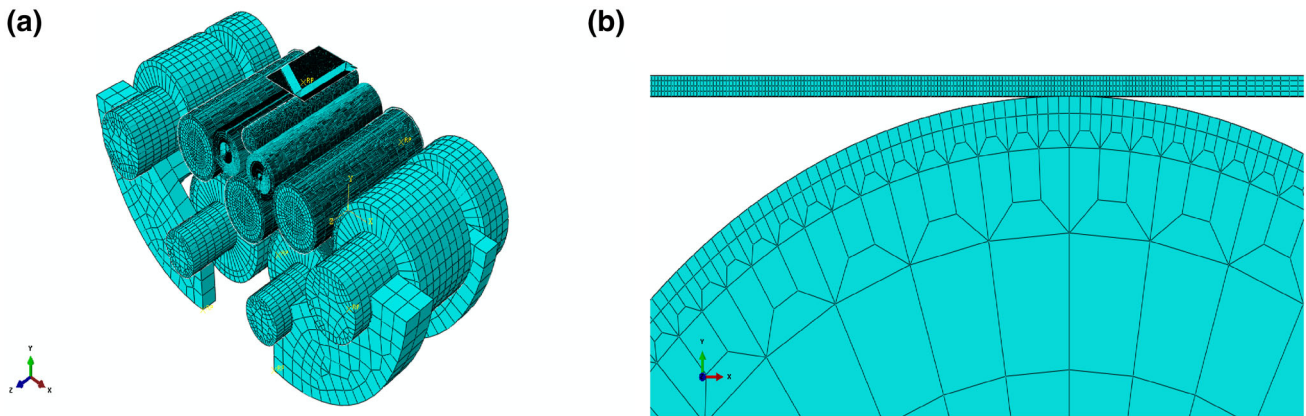


Fig. 11 Three-dimensional model for 20-high mill. **a** A complete model; **b** drawing of partial enlargement

The comparisons of FEA results with the experimental results are shown in Fig. 13. In Fig. 13a, strip entry thickness and width are 0.3 mm and 85 mm, respectively; front and back tensions are 118 MPa/118 MPa; there are

two taper at both ends of the first intermediate roll, with taper angle of 0.003 and taper length of 50 mm. The FEA result for the 21.1% reduction is compared to the experimental result for the 20.2% reduction. In Fig. 13b, strip entry thickness is 0.2 mm, and strip width is 85 mm; front and back tensions are 118 MPa/118 MPa; there are two taper setups at both ends of the first intermediate roll, with taper angle of 0.002 and taper length of 50 mm. The FEA result for the 16.9% reduction is compared to the experimental result for the 17.7% reduction. The comparisons show that the FEA results are consistent with the measured results, proving that the test method is true and reliable. Figure 13 also shows that the metal flows from a region with a small tension to a region with a large one inside; therefore, there is a negative displacement in the middle zone of the strip. However, the effect of the edge drop of strip on the metal flow is greater than that of the tension in the strip edge. Therefore, there is a significant positive displacement at the extreme edge.

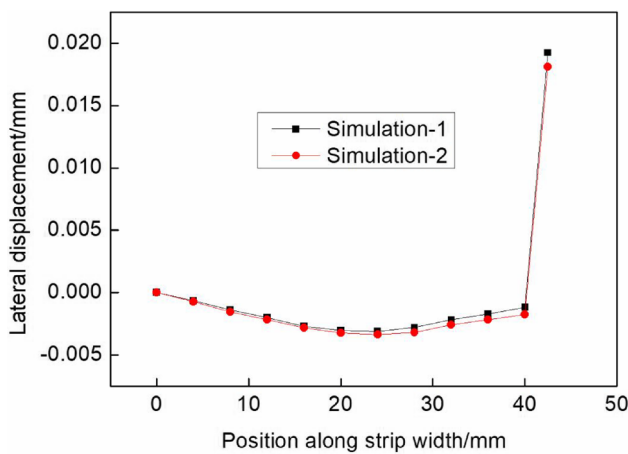


Fig. 12 Comparison result under different grid sizes

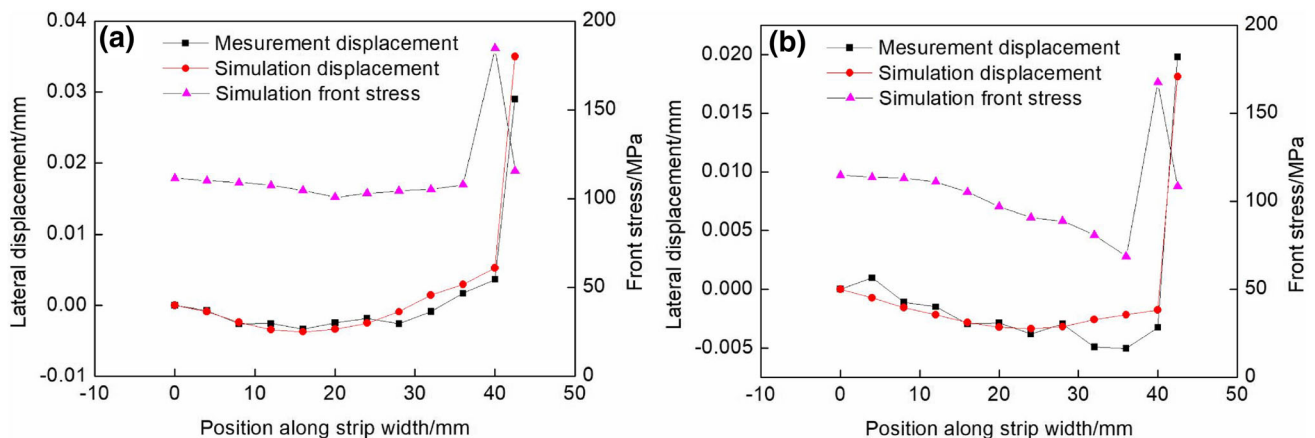


Fig. 13 Comparisons between FEA and experimental results. **a** 0.3 mm thick strip; **b** 0.2 mm thick strip

5 Conclusions

Grids with line thickness of 10 μm and clear boundaries were successfully manufactured on the strip surface by lithography. Afterward, the effects of the reduction, the front and back tensions, and the first intermediate roll taper angle on the metal lateral flow were analyzed. With the increase in the reduction and the decrease in the taper angle and tension, the results show that the thinning phenomenon becomes more serious at the edge and the lateral displacement is changed from negative to positive.

The strip shape was calculated with and without considering the lateral displacement of the metal, and the calculated results were compared with the measurements. It is found that the results with the consideration of the lateral displacement are closer to the measurements. Thus, it can be concluded that the lateral displacement is critical to the shape control.

The comparisons show that the FEA results are consistent with the measured results, proving that the test method is reliable.

Acknowledgements The authors gratefully acknowledge the support of the National Natural Science Foundation of China (51474190), Natural Science Foundation of HeBei Province (E2015203311), and Taiyuan City Science and Technology Major Projects (170203).

References

- [1] T. Von Karman, *Z. Angew. Math. Mech.* 5 (1925) 139–141.
- [2] E. Orowan, *Proc. Inst. Mech. Eng.* 150 (1943) 140–167.
- [3] P. Hartley, C.E.N. Sturgess, C. Liu, G.W. Rowe, *Int. Mater. Rev.* 34 (1989) 19–34.
- [4] H. Matsumoto, *ISIJ Int.* 31 (1991) 550–558.
- [5] A.E. Dixon, W.Y. Daniel Yuen, *Steel Res. Int.* 79 (2008) 287–296.
- [6] H. Furumoto, K. Yamada, J. Yanagimoto, *ISIJ Int.* 42 (2002) 736–743.
- [7] S. Serajzadeh, Y. Mahmoodkhani, *Int. J. Mech. Sci.* 50 (2008) 1423–1431.
- [8] J.H. Ruan, L.W. Zhang, Z.G. Wang, T. Wang, Y.R. Li, Z.Q. Hao, *Ironmak. Steelmak.* 42 (2015) 585–593.
- [9] C.W. Li, X.C. Wang, Q. Yang, L.S. Wang, *J. Univ. Sci. Technol. Beijing* 35 (2013) 222–227.
- [10] S.I. Oh, S. Kobayashi, *Int. J. Mech. Sci.* 17 (1975) 293–305.
- [11] K.F. Kennedy, *J. Eng. Ind.* 109 (1987) 248–256.
- [12] R.E. Johnson, *Int. J. Mech. Sci.* 33 (1991) 449–469.
- [13] Y. Liu, J. Lian, *Advances in engineering plasticity and its applications*, Elsevier, Amsterdam, 1993.
- [14] D. Yun, D. Lee, J. Kim, S. Hwang, *ISIJ Int.* 52 (2012) 1109–1117.
- [15] D.H. Lee, K.B. Lee, J.S. Lee, S.J. Yun, T. J. Shin, S.M. Hwang, *J. Manuf. Sci. Eng.* 136 (2014) 051014.
- [16] C.W. MacGregor, L.F. Coffin Jr., J.C. Fisher, *J. Appl. Phys.* 19 (1948) 291–297.
- [17] C.P. Burger, H.A. Gomide, *Exp. Mech.* 22 (1982) 441–447.
- [18] P.F. Thomson, J.H. Brown, *Int. J. Mech. Sci.* 24 (1982) 559–576.
- [19] Y.J. Liu, A.K. Tieu, D.D. Wang, W.Y.D. Yuen, *J. Mater. Process. Technol.* 111 (2001) 142–145.